

# Detection and Characterization of Defect in Carbon Fiber Reinforced Composite Laminate Using Passive Thermography

Saran Kumar Sekar<sup>1</sup>

<sup>1</sup>Lecturer, Department of Aeronautics, St. Theresa International College, Nakhonnayok-Thailand

## Article Info

Volume 83

Page Number: 2195 - 2201

Publication Issue:

May - June 2020

## Abstract:

Real-time non-destructive assessment is important during load testing of composites. Overlay for rising use of Carbon Fiber Reinforced Polymer (CFRP), the fast, visible, and free of Interference technique for discovering mechanical influence deterioration is critical requirement. The main concept of the research experiment using passive thermography is to locate the damaged areas during polymer deformation using the energy release. The test specimens were established over the temporal and spatial temperature distribution. Based on that, the forms of CFRP impact damage are described. The purpose of this paper is to use thermography and Ultrasonic to classify the types of impact damages. The results obtained show that under the different impact energies various types of impact damage occur and can be defined in the thermographic picture. Based on the fiber composite material used CFRP, Material thickness and impact energy a measure of sensitivity of the detection of these methods for the different damages is performed in this paper. The methods of thermography analysis used after the damage are complemented by high-temporal resolution thermography measurements, which are documented during the effect. The investigations of the impact damaged CFRP test specimens with thermography show that kind and shape of the damage. In the test specimens, a defined large crack can be detected which has spread parallel to the course of the fibers of the layer of the laminate. To this end, various specimens undergo impact testing with different energies of five, ten, fifteen, twenty, thirty, and thirty six Joule and monitored by infrared camera. Information handling procedures are obtainable which facilitate recognition of the minor changes thermo-graphic waveforms resultant by defect development in actual phase. The findings of the passive thermography measurements are compared with the validation ultrasonic measurements.

**Keywords:** Ultrasonic, Detection, Non-destructive testing, CFRP laminate, Passive Thermography

## Article History

Article Received: 11 August 2019

Revised: 18 November 2019

Accepted: 23 January 2020

Publication: 10 May 2020

## 1. INTRODUCTION:

CFRP composite overlay materials is commonly used in mechanical applications, for example, aviation, car, wind and railroads because of their amazing presentation of high explicit quality and unbending nature, high plan capacity, high fatigue obstruction and high corrosion opposition over numerous other material sorts. The key disadvantages of CFRP composite materials, be that as it may, is their poor impact opposition; in reality, CFRP composite materials are inclined to affect during the creation, administration and fix cycle,

brought about by such mechanical effect sources as falling gear, overwhelming storms and stones. In this manner, recognizing mechanical effect defect so as to encourage the consequent fixes is of significance. When optoelectronic research advances, infrared thermography is regarded as a promising, non-ruinous localization strategy because of the benefits of rapid, non-contact, wide region assessment and visual outcomes and so forth., which includes two methodologies: dynamic and aloof all through thermography discovery. Reason dynamic thermography is normally implemented to identify the structures in

the upkeep stage just as the techniques for discovery referenced in, which are not appropriate for constant location. Albeit uninvolved thermography utilizes an infrared camera to imagine an item's temperature varieties without outer warm boost, this method demonstrates perfect for ongoing location. Most definitely, it can meet the accompanying prerequisites: i) constant following, (ii) Clean and non-contact, (iii) fast and visual position, and (iv) wide region inclusion. Consequently the mechanical effect defect of composite CFRP overlays was portrayed right now. To this end, the vitality transformation was concentrated during sway case, which established the framework for distinguishing sway defect of CFRP cover utilizing aloof thermography. Right now, examples are subject with various energies to the effect test and are followed progressively by an infrared camera. In synopsis, inactive thermography gives a promising option in contrast to traditional non-ruinous test strategy by imaging the varieties in surface temperature of curios exposed to dynamic burden. Inactive thermography does not assume regulation of the vitality applied, for example, the light, the warm air, the diminishing moisture, and the piling of basics. Infrared (IR) camera tracks the thermal symbolism inactively. An example of the various examinations performed utilize detached thermography for defect discovery during cyclic exhaustion auxiliary stacking is to Distinguish the no monotonous, low, transient thermal signals produced. Past experiments were carried out using latent thermography during static stacking on metals, composites reinforced with glass fiber, and composites with carbon fiber.

## 2. Hypothetical Basics

The example's energy transformation is set out in Figure 1 during the impact occasion. Suppose the head of the pendulum hits the example using a specific speed,  $C_1$  as an outcome, it is re-bounded by the sample with second specific speed  $C_2$ . As per the energy balance condition the misfortune active

energy,  $J_i$ , which is consumed by the example, can be gotten as appeared in condition (1),

$$J_i = \frac{1}{2} W C_1^2 - \frac{1}{2} W C_2^2 \quad (1)$$

Where,  $W$  is the pendulum head number, the  $J_i$  is absorbed by a triple function specimenis given by equation (2),

$$J_i = J_p + J_v + J_d \quad (2)$$

Where  $J_p$  is the plastic deformation energy,  $J_v$  is sample vibrational energy,  $J_d$  is the damage energy

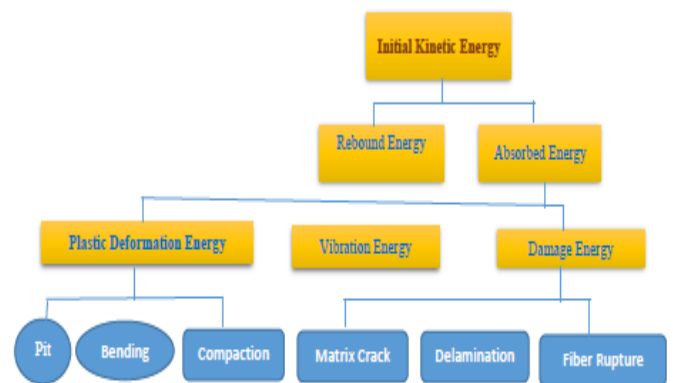


**Figure 1.** Energy conversion during impact experience on specimen

## 3. EXPERIMENTAL DETAILS

### 3.1 MATERIAL AND EQUIPMENT

The examined examples right now made of CFRP cover, stretched out in  $[46^\circ/0^\circ / -46^\circ/89^\circ]_{3,99s}$  and stacked in Thirty two layers, 149 mm x 99 mm x 5 mm in thickness, which have been carefully done ex-manufacturing plant location utilizing ultrasonic staged exhibit innovation to guarantee the integrity.

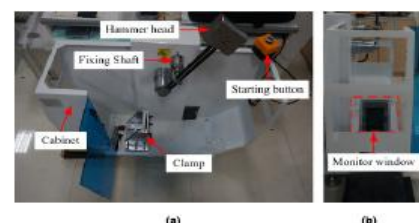


**Figure 2.** (i) Impact strategies. (ii) Observing window.

Illustration. 2 Standardized impact check gadget reveals itself. At Fig. 2(i) the pure pendulum head is used to reach the specimen where the heap sensor and the vibrating sensor are mounted to collect correlative information, such as contact strength, pace et al and some string gaps to include or decrease the tempered steel blockchanging the heaviness of the pendulum head to alter the vitality effect. The dynamic vitality of the pendulum head is determined by the impact vitality. The heavier pendulum head displays the higher impact vitality along these lines; the fixing shaft works in this with double power: Fixing of the pendulum head when measuring the impact and determining the underlying stature of the pendulum head; using the brace to speed up the example. In addition, the impact gadget and clip are placed in the desktop to forestall the impact instigated slag to sputter around.

The infrared camera is positioned in Fig, at the search window. 2 (ii), to provide an illustration of the surface temperature area. The infrared camera distinguishes the temperature spectrum from -39 °C to 1190 °C with an affectability of 0:029 °C at 29 °C, sensitivity of 1.99 percent perusing, targets of 639 x 479 dots, operating in the 7.49 – 13.9 μm infrared band spectrumand Full information grab speed of 50 frames per second [25].

### 3.2 INVESTIGATIONALTECHNIQUES

As seen, this research focuses on the identification of impact defects and the representation of CFRP overlays using uninvolved thermography by estimating the surface temperature. We use the gadget for pendulum sway in Fig. 2 to re-enact the cause of the outside influence.The impact test is performed using 22.9°C room temperature and 29.99% humidity.The infrared camera is positioned at the screen window during the impact procedure, fig 2 (ii) the subtleties of the constant observation and of the related technique shall be reported as the accompanying five phases.

- **Stage 1:**Coating the example surface with a thin layer of dissolvable dark paint to increase the intensity of infrared radiation and correct the example in the clamp.

- **Stage 2:**Starting the infrared camera, adjusting the central separation to enable the recording of fair example grouping of warm pictures and directing non-consistency adjustment of the infrared camera.
- **Stage 3:**Documenting the surface temperature shift of example when the impact happens, and performing similar investigation, sooner or later documenting and saving the warm picture grouping of example until the pendulum head tumbling off.Squeezing the startup catch to make the pendulum head tumble off the fixing shaft at that point, and hitting the example. The pendulum head is man-made controlled when bounced back, to forestall various effects on the example.
- **Stage 4:**Adjusting the pendulum head heaviness to change the vitality effect and rehabilitating over three phases. Examples with the quantity of # 1-# 6 are now subjected to the impact test with specific energies of five Joule, ten Joule, fifteen Joule, twenty Joule, thirty Joule and thirty six Joule.
- **Stage 5:**Recognizing all the tried examples.

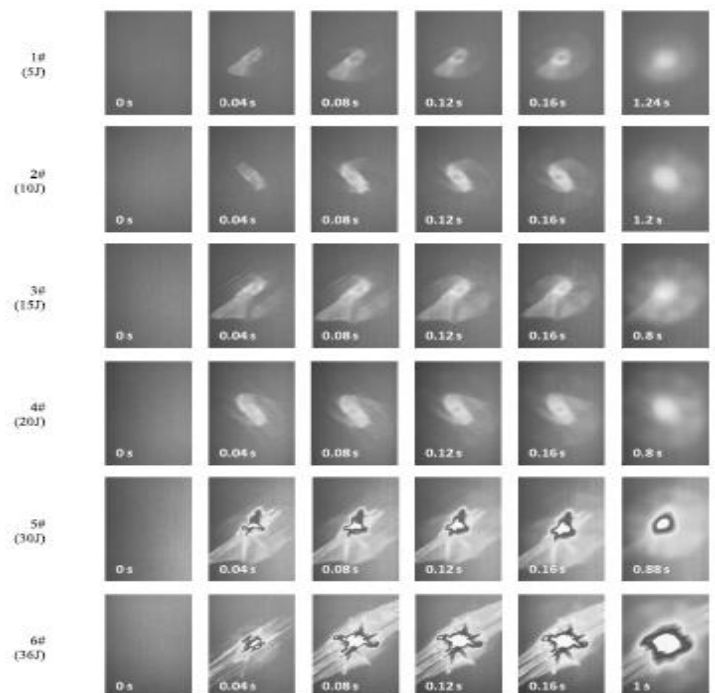


Figure 3. Series of thermal images captured by an infrared camera.

The accumulated picture outlines are set of eight hundred and the chronicle recurrence is set at twenty five hertz, i.e., each edge of thermography picture is assembled each 1/24 seconds and complete social occasion time is thirty two seconds in the detached thermography. The test subtleties are recorded in table I.

TABLE I. Experimental details.

| Samples | Impact energy (J) | Footagerate (Hz) | Collected frames |
|---------|-------------------|------------------|------------------|
| #1      | 5                 | 25               | 800              |
| #2      | 10                | 25               | 800              |
| #3      | 15                | 25               | 800              |
| #4      | 20                | 25               | 800              |
| #5      | 30                | 25               | 800              |
| #6      | 36                | 25               | 800              |

## 4. EXPERIMENTAL RESULTS

### 4.1 Tests Using Passive Thermography

On sway occasion, the variable surface temperature using an infrared camera is measured and the comparative thermography image arrangement of examples with different energies appears in Fig. 3. At Fig. 3, Due to the effect caused by heat dispersion, the temperature of the problem area in the impact zone is higher than that of the sound region which can be used to detect the impact defect. There are also some significant wonders to be identified and investigated from the grouping of pictures, reported as follows:

a) If the pendulum head does not touch the example yet, then there is no proximity of the problem area in the thermography picture; all things considered, the surface temperature of the examples shows extraordinary (i.e., the proximity of the characteristic region and dull territory to the example surface) in view of the natural interference and the surface qualities of the example. The problem area along the heading of the fiber layer (appears to grid splitting) appears right off the one with a straight line form at 1/24 seconds. Immediately thereafter, the problem area starts to expand windingly (appears to

delamination), until at 1/6 seconds, a circular hot spot is formed.

- b) Using a specified effect vitality, for example the picture arrangement of example #1 with sway vitality of five Joule, the problem area close by the effect point is more brilliant than that of somewhere else, showing temperature in this is higher, which might be because of the pressure fixation and the event of network splitting and delamination actuated by sway occasion.
- c) The problem area with higher effect vitality is more brilliant than that with lower sway vitality at a similar minute. Since the effect defect is increasingly genuine under the higher effect vitality, subsequently, the more warmth is dispersed and Prompts an example of a higher surface temperature.
- d) In the picture succession of examples #1 - #4, there is the nearness of a relative dim point in the focal point of problem area and the reasons are fundamentally gotten from that effect actuated pit prompts the decrease of thickness and the expansion of the nearby thickness, as per the condition,  $\alpha = k/\rho c$ , the comparing warm dispersion proficiency,  $\alpha$ , diminishes with the expansion of thickness,  $\rho$ , therefore, the capacity to will in general warmth balance decays. While in the picture arrangement of examples #5 - #6, no dull point yet more brilliant problem area (for example white spot) shows up, which demonstrates that the dispersed warmth increments pointedly under effect vitality from twenty Joule to thirty Joule. The explanation prompting this wonder is connected with the event of fiber crack that discharges copious warmth under bigger effect vitality.

Heat dispersal, which prompts the variable temperature on the example surface, is linked to the event of impact defect. In this way, the analysis of surface temperature can facilitate an understanding of the portrayal of impact defects. On this list, the information about surface temperature is investigated. In order to evacuate the effects of condition meddle and the surface attributes of example superficial temperature, the temperature

comparison, is currently being used to investigate the variable temperature that can be measured using Eq. (3).

$$\Delta\tau_t = \tau_t - \tau_0 \quad (3)$$

Where,  $\tau_t$  and  $\tau_0$  represent surface heat at the period of  $t$  and 0 respectively, and  $\Delta\tau_t$  is the heat variance at the period of  $t$ .

Two zones called P1 and P2 are identified individually in the defect territory and sound zone and  $\Delta\tau$  subtracts the mean temperature between area P1 and zone P2. The bends of  $\Delta\tau$  versus  $\tau$  of examples with various effect energies is acquired utilizing Eq. (3), as appeared in Fig. 4. The  $\Delta\tau$  stays unaltered with the estimation of 0 °C at  $\tau < 0$  s, when the pendulum head doesn't hit the example. While, the  $\Delta\tau$  out of nowhere increments at  $\tau > 0$  s when the pendulum head hits the example to discharge warmth and afterward the  $\Delta\tau$  bit by bit diminishes because of the warmth trade with encompassing condition. The vaporous  $\Delta\tau$  decline marvel is available since the example surface responds to the effect in a versatile way (thermo-flexible impact) and the quick  $\Delta\tau$  increment wonder is because of the plastic response of example to affect occasion (thermo-plastic impact) in fig. 5.

The greatest extraordinary surface temperature  $\Delta\tau_{max}$  between P1 region and P2 region is plotted against sway vitality to examine the temperature changes under various impact energies in Fig. 6.

From Fig. 6, we can find that when the effect vitality is under twenty Joule, the  $\Delta\tau_{max}$  builds relative easily however under one and half °C, while when the effect vitality ranges to thirty Joule and thirty six Joule, the  $\Delta\tau_{max}$  spans to ten °C and twenty four °C separately, which demonstrates the  $\Delta\tau_{max}$  shows a nonlinear relationship with sway vitality. In detail, there might be the nearness of solid increment of  $\Delta\tau_{max}$  under some effect vitality between twenty Joule and thirty Joule, which is steady with marvels 3) and 4) and the explanation might be relative with the difference in sway defect types, i.e., network squeaking and delamination are the main forms of swaying defects when the impact vitality is below 20 Joule while the fiber breakage happens and goes with plenteous warmth dissemination when the effect vitality ranges to thirty Joule and thirty six Joule.

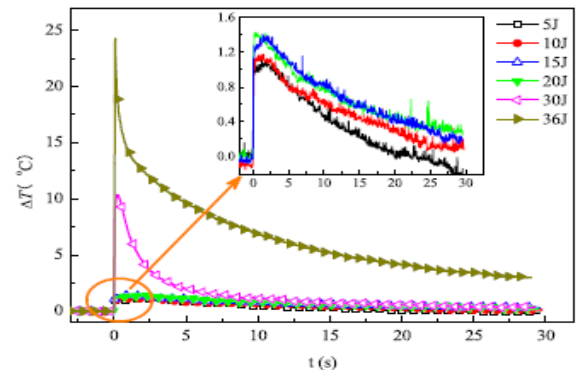


Figure 4. Example curves of surface temperature evolution.

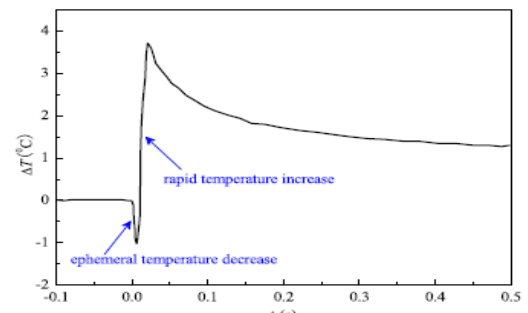


Figure 5. In the event of impact the ephemeral temperature decreases.

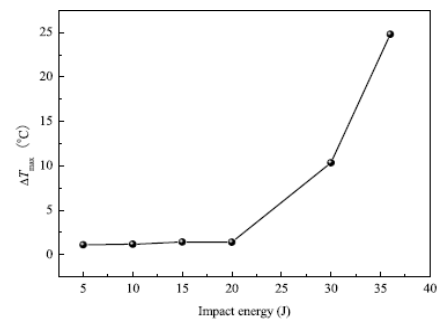


FIGURE 6.  $\Delta\tau_{max}$  for the species under different energy impacts.

## 4.2 IMPACT DAMAGE CHARACTERIZATION

The characterization of forms of impact damage in passive thermography is described in the table II in overall.

TABLE II. Description of impact damage in passive thermography.

| Impact Damage  | Characterization in Thermography Image        |
|----------------|---|
| MatrixCracking | Straight line shape in fiber path of Hot spot |
| Delamination   | Asymmetrical block form of Hot spot           |

|               |   |
|---------------|---|
| Fiber rupture | Conventional line form perpendicular to the fiber way of Hot spot |
|---------------|---|

## CONCLUSION

Right now, point is to portray the effect defect types utilizing latent thermography. To this objective, a few examples are initially exposed to forcefully affect test with various energies and ongoing distinguished utilizing aloof thermography. At that point, the location results are investigated to understand the portrayal of effect defect types. The got outcomes show that distinctive effect defect types happen under the diverse effect vitalities. In detail, when the effect vitality is small, the effect defect forms include network splitting and delamination when the effect vitality is massive, the fiber burst happens despite the frame breaking and delamination. Effect forms of defects are represented in inactive thermography on this assumption. The frame splitting and fiber crack are represented individually as a problem area using traditional link type with the fiber heading and opposite to the fiber path, whereas the delamination can be defined as a problem area with sporadic square shape, That can promote identifiable evidence of mode of effect defect and an evaluation of degree of defect. It is crucial that this work is conceivably intended to determine the relation between the types of defects and the energy effects. But further studies are required to find the energy threshold between different types of damage.

## REFERENCES

[1] Joseph Zalameda and William Winfree, "Detection and Characterization of Damage in Quasi-Static Loaded Composite Structures Using Passive Thermography," Article in Sensor Journal, Sensors 2018, 18, 3562; doi: 10.3390/s18103562.

[2] M. K. Bannister, "Development and application of advanced textile composites," *J. Mater. Des. Appl.*, vol. 218, no. 3, pp. 253-260, 2004.

[3] T.-W. Shyr and Y.-H. Pan, "Impact resistance and damage characteristics of composite laminates," *Compos. Struct.*, vol. 62, pp. 193-203, Nov. 2003.

[4] M. Castaings, D. Singh, and P. Viot, "Sizing of impact damages in composite materials using ultrasonic guided waves," *NDT & E Int.*, vol. 46, pp. 22-31, Mar. 2012.

[5] S. C. Garcea, Y. Wang, and P. J. Withers, "X-ray computed tomography of polymer composites," *Compos. Sci. Technol.*, vol. 156, pp. 305-319, Mar. 2018.

[6] M. S. Sohn, X. Z. Hu, J. K. Kim, and L. Walker, "Impact damage characterization of carbon fiber/epoxy composites with multi-layer reinforcement," *Compos. B, Eng.*, vol. 31, no. 8, pp. 681-691, 2000.

[7] T. Chady, P. Lopato, and B. Szymanik, "Terahertz and thermal testing of glass-fiber reinforced composites with impact damages," *J. Sensors*, vol. 2012, Feb. 2012, Art. No. 954867. doi: 10.1155/2012/954867.

[8] N. Liu, Q. M. Zhu, C. Y. Wei, N. D. Dykes, and P. E. Irving, "Impact damage detection in carbon fiber composites using neural networks and acoustic emission," *Key Eng. Mater.*, vol. 167, pp. 43-54, Jun. 1999.

[9] M. Saeedifar, M. A. Najafabadi, D. Zarouchas, H. H. Toudeshky, and M. Jalalvand, "Clustering of interlaminar and intralaminar damages in laminated composites under indentation loading using Acoustic Emission," *Compos. B, Eng.*, vol. 144, pp. 206-219, Jul. 2018.

[10] T. Wandowski, P. H. Malinowski, and W. M. Ostachowicz, "Delamination detection in CFRP panels using EMI method with temperature compensation," *Compos. Struct.*, vol. 151, pp. 99-107, Sep. 2016.

[11] W. Harizi, S. Chaki, G. Bourse, and M. Ourak, "Mechanical damage assessment of polymer matrix composites using active infrared thermography," *Compos. B, Eng.*, vol. 66, pp. 204-209, Nov. 2014.

[12] W. Harizi, S. Chaki, G. Bourse, and M. Ourak, "Mechanical damage assessment of glass fiber-reinforced polymer composites using passive infrared thermography," *Compos. B, Eng.*, vol. 59, pp. 74-79, Mar. 2014.

[13] K. Zheng, Y.-S. Chang, K.-H. Wang, and Y. Yao, "Improved nondestructive testing of carbon fiber reinforced polymer (CFRP) composites using pulsed thermograph," *Polym. Test.*, vol. 46, pp. 26-32, Sep. 2015.

- [14] Y. He, S. Chen, D. Zhou, P. Wang, and S. Huang, "Shared excitation based nonlinear ultrasound and vibro-thermography testing for CFRP barely visible impact damage inspection," *IEEE Trans. Ind. Informat.*, vol. 14, no. 12, pp. 5575-5584, Dec. 2018. doi: 10.1109/TII.2018.2820816.
- [15] V. Arora, J. A. Siddiqui, R. Mulaveesala, and A. Muniyappa, "Pulse compression approach to non-stationary infrared thermal wave imaging for nondestructive testing of carbon fiber reinforced polymers," *IEEE Sensors J.*, vol. 15, no. 2, pp. 663-664, Feb. 2015.
- [16] J. A. Siddiqui, V. Arora, R. Mulaveesala, and A. Muniyappa, "Infrared thermal wave imaging for nondestructive testing of fibre reinforced polymers," *Experim. Mech.*, vol. 55, no. 7, pp. 1239-1245, 2015.
- [17] T. Liang, W. Ren, G. Y. Tian, M. Elradi, and Y. Gao, "Low energy impact damage detection in CFRP using eddy current pulsed thermography," *Compos. Struct.*, vol. 143, pp. 352-361, May 2016.
- [18] A. Foudazi, I. Mehdipour, K. M. Donnell, and K. H. Khayat, "Evaluation of steel fiber distribution in cement-based mortars using active microwave thermography," *Mater. Struct.*, vol. 49, no. 12, pp. 5051-5065, Dec. 2016.
- [19] T. Li, D. P. Almond, and D. A. S. Rees, "Measurement Science and Technology Crack imaging by scanning laser-line thermography and laserspot thermography," *Meas. Sci. Technol.*, vol. 22, no. 3, pp. 407-414, 2011.
- [20] S. Bagavathiappan, B. B. Lahiri, T. Saravanan, T. Jayakumar, and J. Philip, "Infrared thermography for condition monitoring\_A review," *Infr. Phys. Technol.*, vol. 60, pp. 35-55, Sep. 2013.
- [21] A. Rogalski, "Infrared detectors: An overview," *Infr. Phys. Technol.*, vol. 43, pp. 187-210, Jun. 2002.
- [22] C. Meola and G. M. Carlomagno, "Infrared thermography of impactdriven thermal effects," *Appl. Phys. A*, vol. 96, pp. 759-762, Aug. 2009.
- [23] C. Meola and G. M. Carlomagno, "Impact damage in GFRP: New insights with infrared thermography," *Compos. A, Appl. Sci. Manuf.*, vol. 41, pp. 1839-1847, Dec. 2010.
- [24] C. Meola et al., "New perspectives on impact damaging of thermoset- and thermoplastic-matrix composites from thermographic images," *Compos. Struct.*, vol. 152, pp. 746-754, Sep. 2016.
- [25] Y. Li et al.: Detection and Characterization of Mechanical Impact Damage Within Multi-Layer Carbon Fiber Reinforced Polymer (CFRP) Laminate Using Passive Thermography," *IEEE Access*, volume 7, pp 27689 – 27698, March 2019.